MOLECULAR AND CELLULAR BIOLOGY, Aug. 2004, p. 6665–6675 Vol. 24, No. 15
0270-7306/04/$08.00+0 DOI: 10.1128/MCB.24.15.6665–6675.2004

Nucleotide Exchange Factor ECT2 Interacts with the Polarity Protein Complex Par6/Par3/Protein Kinase Cζ (PKCζ) and Regulates PKCζ Activity

Xiu-Fen Liu,† Hiroshi Ishida,‡ Razi Raziuddin,† and Toru Miki*

Molecular Tumor Biology Section, Basic Research Laboratory, National Cancer Institute, Bethesda, Maryland 20892-4255

Received 25 September 2003/Returned for modification 21 November 2003/Accepted 12 May 2004

Regulation of cell polarity is an important biological event that governs diverse cell functions such as localization of embryonic determinants and establishment of tissue and organ architecture. The Rho family GTPases and the polarity complex Par6/Par3/atypical protein kinase C (PKC) play a key role in the signaling pathway, but the molecules that regulate upstream signaling are still not known. Here we identified the guanine nucleotide exchange factor ECT2 as an activator of the polarity complex. ECT2 interacted with Par6 as well as Par3 and PKCζ. Coexpression of Par6 and ECT2 efficiently activated Cdc42 in vivo. Overexpression of ECT2 also stimulated the PKCζ activity, whereas dominant-negative ECT2 inhibited the increase in PKCζ activity stimulated by Par6. ECT2 localization was detected at sites of cell-cell contact as well as in the nucleus of MDCK cells. The expression and localization of ECT2 were regulated by calcium, which is a critical regulator of cell-cell adhesion. Together, these results suggest that ECT2 regulates the polarity complex Par6/Par3/PKCζ and possibly plays a role in epithelial cell polarity.

Cell polarization is fundamental for a variety of biological processes, including asymmetrical cell division, directional cell migration, and establishment and maintenance of apical-basal polarity in epithelial cells (4, 6, 23, 29). In recent years, the molecular mechanisms underlining cell polarity have begun to be understood. A central participant is the evolutionarily conserved multiprotein complex Par3/Par6/atypical protein kinase C (aPKC), which is crucial for anterior-posterior polarity in *Caenorhabditis elegans* and the apical-basal polarity of epithelial cells and neuroblasts in *Drosophila melanogaster* (3, 4). The polarity complex also plays essential roles in assembling and regulating tight junction formation in mammalian epithelial cells (9, 16, 25, 42, 43).

Genetic analyses in *C. elegans* identified six Par proteins (Par 1 to 6) and aPKC as key components of the molecular machinery required for anterior-posterior development. In *par6* mutants, blastomeres of equal size are generated, but subsequent asymmetric cell divisions are not observed (39). The *Drosophila* orthologue of *C. elegans* Par6 is essential for asymmetric division on the formation of neuroblasts. Similarly, in mammalian epithelial cells, Par6 is necessary for establishing basolateral and apical surfaces in epithelial cells (24, 42), cell polarity in rat astrocyte migration (5, 7), and axon formation in neuron development (34). Recently, Par6 and aPKC were reported to regulate other two polarity complexes, mLgl/Dlg/Scrib (25, 43) and Pals/PATJ/Crumbs (9).

Tight junctions function as one of the intercellular barriers to regulate paracellular permeability in vertebrate epithelial and endothelial cells. They also provide physical fences within the membrane bilayer that prevent intermixing of membrane proteins and thus maintain cell surface asymmetry. Furthermore, they provide the essential structures and serve as specific sites for vesicle targeting to establish and maintain the epithelial polarity of the cell membrane (14, 18). Tight junctions are composed of large complexes of cytoplasmic and membrane proteins. Adapters, such as ZO proteins, and signaling molecules, such as small GTPases, are components of the complexes (8, 15, 28, 33, 35). Additionally, Par6, Par3, and aPKCs localize to tight junctions in Madin-Darby canine kidney (MDCK) cells (23, 42, 43). Activation of Par6 or overexpression of aPKC regulates the formation of tight junctions.

The scaffolding protein Par6 contains a single PDZ (PSD95/Dlg/ZO-1) domain that interacts with the N-terminal PDZ domain of Par3, which contains three PDZ domains. Its N-terminal PB1 (Phox and Bem1p) region can heterodimerize with the complementary PB1 domain of aPKC to regulate aPKC function. The Par6 PB1 domain is followed by the CRIB motif, which associates with the GTP-bound forms of the Rho GTPases Cdc42 and Rac1 (6, 23, 26, 38, 43).

Rho GTPases, represented by RhoA, Cdc42, and Rac1, are molecular switches that regulate a wide range of cellular responses, including reorganization of cytoskeleton, mitogenic signaling, cell cycle progression, membrane trafficking, and cell polarity (8, 12, 22, 33, 38, 41). The biological activities of Rho GTPases depend on cycling between the active GTP-bound state and the inactive GDP-bound state. The GTP-bound forms of Rho proteins can specifically interact with their effectors or targets and transmit signals to downstream molecules. Turning on the switch requires the displacement of GDP by GTP, which is promoted by guanine nucleotide exchange factors. The signal is terminated by GTPase-activating proteins

* Corresponding author. Mailing address: Molecular Tumor Biology Section, Laboratory of Cell Biology, National Cancer Institute, Building 37, Room 2144, 37 Convent Dr., MSC 4255, Bethesda, MD 20892-4255. Phone: (301) 496-2289. Fax: (301) 496-2215. E-mail: toru@helix.nih.gov.

† Present address: Laboratory of Cell Biology, National Cancer Institute, Bethesda, MD 20892-4255.

‡ Present address: Division of Experimental Therapeutics, Walter Reed Army Institute of Research, Silver Spring, MD 20910.

through hydrolysis of GTP, returning the GTPase to the GDP-bound state. The Dbl family guanine nucleotide exchange factors provide exquisite control over the signaling event mediated by the Rho GTPases (2, 19, 40).

One of the Dbl family members, ECT2, was previously isolated in a search for mitogenic signal transducers in epithelial cells (20). ECT2 contains the Dbl homology and pleckstrin homology domains, which are the hallmarks of Rho guanine nucleotide exchange factors, and injection of ECT2 transfectants into nude mice efficiently induces tumor formation (21). The N-terminal half of ECT2 contains cell cycle regulator-related domains, including two tandem repeats of the BRCA-1 C-terminal domain (31). Removal of the N-terminal half of ECT2 strongly activates its transforming activity in NIH 3T3 fibroblasts by changing its subcellular localization and releasing it from negative regulation (30). Further studies indicated that ECT2 is a guanine nucleotide exchange factor for RhoA, Rac1, and Cdc42 in vitro (37). ECT2 is induced in regenerating mouse liver, and its expression is regulated by serum and growth factors (31, 32). Interestingly, ECT2 localization is cell cycle dependent: ECT2 localizes in the nucleus in interphase and condensed in mitotic spindles in mitosis and then in the midbody during cytokinesis. Inhibition of ECT2 by expression of a dominant negative mutant or microinjection of anti-ECT2 antibody specifically blocks the completion of cytokinesis (37). GTP-bound RhoA is specifically accumulated during cytokinesis, and dominant negative ECT2 inhibits its accumulation (13).

In this study, we identified ECT2-interacting proteins in a yeast two-hybrid system. Surprisingly, one of the ECT2-interacting protein candidates was a cell polarity determinant, Par6. We found that ECT2 and Par6 interact both in vivo and in vitro. We further demonstrated that ECT2 expression regulates aPKC activity. Endogenous ECT2 was detected in cell-cell junctions of MDCK cells. ECT2 expression and junctional localization were regulated by calcium. These results suggest a possible role of ECT2 in tight junction formation.

MATERIALS AND METHODS

Antibodies and reagents. Monoclonal anti-ZO-1 antibody was purchased from Zymed Laboratories (South San Francisco, Calif.). The mouse anti-Flag and anti-Myc antibodies were obtained from Sigma (St. Louis, Mo.) and Santa Cruz Biotechnology (Santa Cruz, Calif.), respectively. Anti-HA monoclonal antibody was from Convance. Anti-maltose-binding protein (MBP) was purchased from New England Biolabs. Polyclonal anti-ECT2 antibody was reported previously (37). Goat polyclonal anti-Par6 (T-20) was obtained from Santa Cruz Biotechnology. Monoclonal anti-glyceraldehyde 3-phosphate dehydrogenase (GAPDH) was purchased from Biodesign Int. Anti-β-tubulin antibody was purchased from Sigma. Human myelin basic protein was obtained from Chemicon International Inc. (Temecula, Calif.). Alexa Fluor 488- or 568-conjugated secondary antibody was purchased from Molecular Probes (Eugene, Oreg.). Horse radish peroxidase-conjugated mouse or rabbit immunoglobulin G (IgG) and enhanced chemiluminescence (ECL) detection regents were from Amersham Bioscience. The Cdc42 activation kit was obtained from Cytoskeleton (Denver, Colo.).

Expression vectors. pGEX2T-Par6A, pGEX2T-Par6B, pGEX2T-Par6C, and Myc-Par3 were gifts from Ian Macara. Flag-Par6A and Flag-Par6C were constructed by subcloning the BamHI/EcoRI fragments into vector pCEV32F3 (30) containing three tandem copies of the Flag epitope at the N-terminal side of the insert. Par6A-N1, Par6A-N2, Par6A-C, Par6C-N, and Par6C-C were generated by PCR and cloned into pCEV32F3. The GFP-Par6B and GFP-Par6C plasmids were constructed by subcloning the full-length Par6 into pEGFP-C1 (Clontech) between the BglII and EcoRI sites. Par6A was similarly cloned into pEGFP-C1 by PCR as a BamHI/BamHI fragment. ECT2 expression plasmids Flag-ECT2-F, Flag-ECT2-N2, Flag-ECT2-N4, Flag-ECT2-ΔN5, GFP-ECT2-ΔN5, and MBP-ECT2-ΔN5 have been described (21, 30, 37). MBP-ECT2-N2 was constructed by replacing the ECT2-ΔN5 fragment with the ECT2-N2 fragment. Myc-ECT2-N4 and Myc-ECT2-ΔN5 were generated by PCR and cloned into the pKmyc expression vector containing the Myc epitope at the N-terminal side of the insert. Hemagglutinin (HA)-tagged PKCζ was a gift from G. Steven Martin.

Two-hybrid assays. ECT2-N2 (residues 1 to 422) was cloned in the bait vector pGilda (Clontech) to express the LexA DNA binding domain (LexA-BD)-ECT2-N fusion protein and used as bait to screen a human testis cDNA library constructed in pB42AD (Clontech). In this system, both the activation domain (AD) vector pB42AD and DNA-binding domain vector pGilda utilize the *GAL1* promoter to drive fusion protein expression under regulation by glucose and galactose in the growth medium. EGY48 yeast cells were transformed by the bait, and library plasmids were transformed with the lithium acetate method. Two-hybrid assays were carried out according to the manufacturer's protocol. Positive clones were selected by His^+ and β-galactosidase activities. The insert of the p42AD plasmids was directly amplified from the yeast colonies by PCR with the vector primers and subjected to sequence analysis.

siRNAs. Double-stranded RNAs of 21 nucleotides were synthesized by Dharmacon Research (Lafayette, Colo.). The RNA sequence used for human ECT2 was taken from positions 638 to 658 relative to the first nucleotide of the start codon (Kamijo et al., unpublished data). Luciferase small interfering RNAs (siRNAs) (GL2; accession no. X65324) served as a negative control. siRNAs were resuspended in RNase-free water at a final concentration of 20 pmol/μl; 15 μl of the stock RNA was mixed with 250 μl of Opti-MEM medium (Gibco, Invitrogen) and transfected by Oligofectamine in 30-mm culture dishes in HeLa cells.

Canine ECT2 cDNA clones were obtained by reverse transcription-PCR with RNA isolated from MDCK cells and primer pairs 5′-ACTAGCTTGGCAGACTC TTC-3′ and 5′-GTGCTTTTGTCTGGATTTTCATCAGC. The ECT2 cDNA clones were obtained from three different reverse transcription-PCRs. A stretch of cDNA containing 1,691 nucleotides was obtained as a partial coding sequence of ECT2 cDNA. This partial canine ECT2 cDNA shares 91% homology with human ECT2 cDNA and 79% with mouse Ect2 cDNA at the nucleotide level. A mixture of four ECT2 siRNAs was designed and used for RNA interference experiments. The sequences of the siRNAs were AAGCCUGGGAAAGGCG GAAUG, AAGAGCUUUAUCAGACUGAAA, AAUGUGUUCAUAGUCA CGGAC, and AAGGCUAAUACUCCUGAGCUC. SiRNAs were transfected with 4 μl of Lipofectamine 2000 in each 12-well culture dish at a final concentration of 50 to 100 nM in calcium-rich medium.

Cell culture and calcium switch assay. Cos7, HeLa, and MDCK cells were grown in Dulbecco's modified Eagle's medium (DMEM) containing 10% fetal bovine serum, 100 U of penicillin per ml, and 100 μg of streptomycin per ml in a humidified chamber under 5% CO_2 at 37°C. Cos7 and HeLa cells were transfected with the Effectene transfection reagent kit (Qiagen). MDCK cells were transfected with Lipofectamine 2000 (Invitrogen Life Technology). For the calcium switch experiments, monolayer cells were washed three times in phosphate-buffered saline (PBS) without Ca^{2+} or Mg^{2+} 5 h after transfection and incubated in low-calcium medium with 2% serum overnight and then switched to normal medium for 4 to 5 h before fixation for immunohistochemistry.

Immunoprecipitation and Western blot analysis. Cos or MDCK cells were washed once with PBS and then lysed in lysis buffer (150 mm NaCl, Triton X-100, 0.05% sodium dodecyl sulfate [SDS], 0.5% sodium deoxycholate, 1% NP-40, 50 mM Tris [pH 7.5], 2 mM EDTA, 10 μg of leupeptin per ml, 2 μg of aprotinin per ml, 20 μM phenylmethylsulfonyl fluoride). Following centrifugation, supernatants were incubated with anti-Flag or anti-Myc monoclonal antibody in lysis buffer for 2 h. Protein G-Sepharose beads were added, and the mixture was incubated for an additional 2 h. The beads were then washed three times with lysis buffer or PBS, and bound proteins were eluted from the beads in SDS sample buffer by boiling for 5 min before separation by SDS-polyacrylamide gel electrophoresis (PAGE). For Western blot analysis, gels were blotted to a polyvinylidene difluoride membrane. Blots were sequentially incubated in 5% milk for 1 h in Tris-buffered saline plus 0.1% Triton X-100, in primary antibody for 1.5 h, and then in secondary antibody for 1 h. After blotting, signals were detected by enhanced chemiluminescence (Amersham BioSciences).

Immunofluorescence and confocal microscopy. Cells grown on coverslips were fixed by methanol or methanol-acetone (1:1) at −20°C for 10 to 30 min. The samples were blocked by 10% fetal bovine serum in PBS for 30 min at room temperature and incubated with primary antibodies against ZO-1 (1:500) or ECT2 (1:250) for 1.5 h in PBS containing 0.1% Tween 20 and 5% fetal bovine serum. The secondary antibody used was either anti-mouse or anti-rabbit IgG conjugated to Alexa Fluor at a dilution of 1:1,000. Coverslips were mounted with Prolong antifade (Molecular Probes). Samples were analyzed and photographed

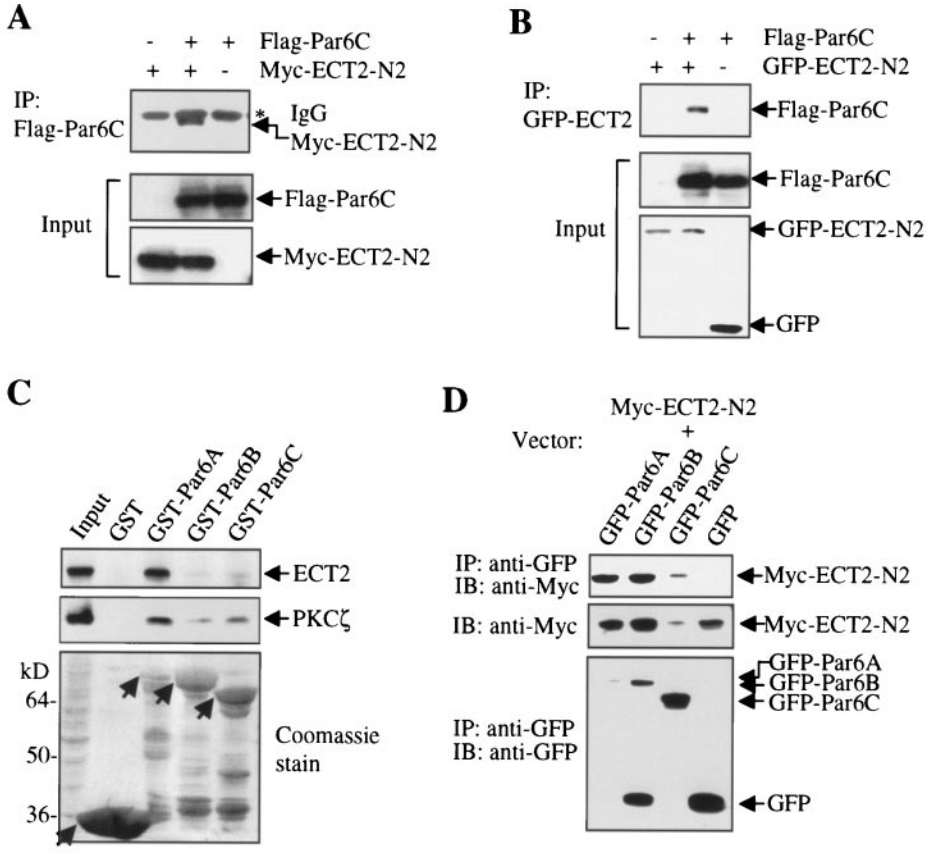

FIG. 1. ECT2 associates with Par6. (A) Lysates from Cos7 cells transfected with Flag-Par6C or empty Flag vector together with Myc-ECT2 or empty Myc vector were immunoprecipitated (IP) and analyzed with anti-Myc or anti-Flag antibody, as indicated. (B) Cos7 cells transfected with Flag-Par6C and GFP-ECT2 or empty GFP vector were lysed and immunoprecipitated by anti-GFP antibody. Western blot analyses were conducted with anti-GFP or anti-Flag antibodies. (C) Equal amounts of MDCK cell lysates were subjected to pulldown assays with GST or GST-Par6. Endogenous ECT2 and PKCζ were detected by immunoblotting with anti-ECT2 and anti-PKCζ antibodies, respectively. A Coomassie stain of the gel to visualize the recombinant proteins is also shown at the bottom. The locations of the bands of the expected sizes are shown by arrows. Note that GST-Par6A was less soluble, and thus the amount of the full-length protein was less than that of the other isoforms. (D) ECT2 associates with Par6 isoforms in vivo. Cos7 cells cotransfected with Myc-ECT2-N2 and GFP-Par6A, -B, or -C expression vectors were lysed and subjected to immunoprecipitation (IP) with anti-GFP antibody. Western blot analysis was carried out with anti-GFP or anti-Myc antibody. The expression level of Myc-ECT2-N2 was reproducibly reduced by the coexpression of GFP-Par6C.

with a Leica DMIRB fluorescence microscope or Zeiss LSM 510 confocal microscope.

In vitro binding assay. For the glutathione *S*-transferase (GST) pulldown assays, 200 to 300 μg of cell lysates was incubated with an excess of GST or GST fusion proteins immobilized to glutathione-Sepharose beads in PBS containing 0.5% Triton X-100 and protease inhibitors (10 μg of leupeptin and 2 μg of aprotinin per ml with 20 μM phenylmethylsulfonyl fluoride) for 1 h at 4°C. Bound proteins were washed three times in PBS plus 0.5% Triton X-100, resolved by SDS-PAGE, and then transferred to a polyvinylidene difluoride membrane. Membranes were probed with anti-ECT2 (1:2,000) or anti-Flag (1:10,000) antibodies. MBP-ECT2-ΔN5 fusion protein was adsorbed to an affinity column containing amylose resin (New England Biolabs) and eluted with 10 μM maltose. Approximately 1 μg of MBP-ECT2-ΔN5 protein was incubated with an excess of GST-Par6A or GST-glutathione-Sepharose beads in PBS plus 0.5% Triton X-100. Detection of MBP-ECT2-ΔN5 was carried out with anti-MBP at a dilution of 1:10,000.

Kinase assays. For the aPKC kinase assay, Cos7 cells were lysed in lysis buffer containing 20 mM Tris-HCl (pH 7.5), 150 mM NaCl, 1% Triton X-100, 1% NP-40, 5 mM EDTA, 1 mM sodium orthovanadate, 1 mM phenylmethylsulfonyl fluoride, 20 μg of aprotinin per ml, 12 mM β-glycerophosphate, 10 mM NaF, and 1 mM sodium orthovanadate. HA-PKCζ was immunoprecipitated with anti-HA antibody, and the beads were washed three times with lysis buffer and then incubated in kinase reaction buffer (20 mM Tris-HCl [pH 7.5], 20 mM $MgCl_2$, 100 μM ATP, and 0.3 μCi of [γ-^{32}P]ATP) for 10 min at 30°C. The reactions were stopped by adding 2× SDS sample buffer and analyzed by SDS-PAGE. Gels were dried and exposed to X-ray film for 24 h.

Cdc42 activation assay. GTP-bound Cdc42 was estimated by the Cdc42 activation kit (Cytoskeleton Inc.). Briefly, HeLa cells were washed with PBS and quickly lysed on ice in the lysis buffer provided by the manufacture. GTP-bound Cdc42 was pulled down by GST-p21 binding domain (PBD) and detected by anti-Cdc42 antibody according to the manufacturer's instructions.

RESULTS

ECT2 interacts with Par6. A yeast two-hybrid screen was carried out to identify proteins that interact with the regulatory domain of ECT2. The N-terminal domain of ECT2 (ECT2-N2, residues 1 to 423) was used as the bait to screen a human testis cDNA library. One of the strongly positive clones was identified as Par6C by sequence analysis following PCR amplification of the insert. The insert contained the entire coding frame of Par6C fused to LexA at the 5′ untranslated region. To verify the interaction of ECT2 with Par6C in mammalian cells, we first expressed Myc-tagged ECT2-N2 and Flag-tagged full-length Par6C in Cos cells and performed coimmunoprecipita-

tion experiments. As shown in Fig. 1A, when Flag-Par6C was immunoprecipitated with anti-Flag antibody, Myc-ECT2-N2 was detected in the complex by anti-Myc antibody. Conversely, when GFP-ECT2-N2 was immunoprecipitated by anti-green fluorescent protein (GFP) antibody, Flag-Par6 was detected by anti-Flag antibody (Fig. 1B). These results suggest that ECT2-N2 interacts with Par6C when expressed in Cos7 cells.

Next, we carried out a pulldown assay to test whether full-length ECT2 interacts with Par6 by using bacterially expressed Par6 fused with GST. As shown in Fig. 1C, endogenous ECT2 in MDCK cells was pulled down by GST-Par6C immobilized on glutathione beads, whereas GST alone did not exhibit detectable association with ECT2. We found that two other Par6 isoforms, Par6A and Par6B, which are encoded by closely related but distinct genes, also associated with ECT2. The interaction of Par6A with ECT2 was most prominent among the Par6 isoforms. We also expressed Myc-ECT2-N2 and GFP-Par6 isoforms in Cos cells and immunoprecipitated the Par6 isoforms with anti-GFP antibody. As shown in Fig. 1D, all three Par6 isoforms were efficiently coimmunoprecipitated by ECT2-N2. To test if endogenous ECT2 interacts with Par6 in vivo, we performed immunoprecipitation experiments (Fig. 2A). When Par6 was immunoprecipitated with anti-Par6 antibody, endogenous ECT2 was detected in the immunoprecipitates, suggesting that ECT2 interacts with Par6 in physiological conditions.

ECT2 associates with PKCζ and Par3. In MDCK cells, Par6 regulates tight junction formation through the binding to aPKC and another polarity determinant, Par3. When Par6 was immunoprecipitated, PKCζ was detected as well as ECT2 in the same immune complex (Fig. 2A). Since we found that the anti-Par6 antibody was not useful in detecting endogenous Par6 in Western blots (data not shown), we could not test the reverse combination. Additionally, when GFP-ECT2-N2, Flag-Par6C, and HA-PKCζ were expressed together in Cos cells, Flag-Par6C and HA-PKCζ were detected in the immunoprecipitates by anti-GFP antibody (Fig. 2B). Interestingly, the association of ECT2 with Par6C was drastically enhanced by the exogenous expression of PKCζ (Fig. 2B, compare lanes 1 and 2). To test whether ECT2 interacts directly with PKCζ, purified PKCζ was pulled down with MBP-ECT2 beads. As shown in Fig. 2C, MBP-ECT2-N2 as well as MBP-Par6A efficiently associated with PKCζ, suggesting that the association is direct. These results indicate that ECT2 is in the Par6/aPKC complex and that the association of ECT2 with Par6 did not exclude the association of PKCζ with Par6.

It is known that another polarity determinant, Par3, associates with Par6 and aPKC and that the Par6/Par3/aPKC complex determines cell polarity (3, 15, 36). To test whether ECT2 also associates with Par3, we transfected Myc-Par3 together with full-length or deletion mutants of Flag-ECT2 and tested the ability of ECT2 derivatives to interact with Myc-Par3. When Myc-Par3 was immunoprecipitated, Flag-tagged full-length ECT2 (Flag-ECT2-F) was detected in the immune complex (Fig. 2D). Conversely, when Flag-ECT2 was immunoprecipitated, Myc-Par3 was detected in the precipitates (data not shown). ECT2-N2 was also coprecipitated with Myc-Par3 (Fig. 2D). However, we could not detect ECT2-N4 (amino acids 1 to 319), which lacks the S domain (see Fig. 4), in the immune complex, suggesting that the S domain is required for the association of ECT2 with Par3.

N-terminal domain of Par6 interacts with ECT2. To define which region of Par6 interacts with ECT2, Myc-ECT2-N2 was coexpressed with Flag-Par6C-N (residues 1 to 247) or Flag-Par6C-C (residues 152 to 345). Par6C-N2 was coimmunoprecipitated with ECT2-N2, whereas Par6C-C was not (Fig. 3A). These results suggest that the N-terminal region of Par6 mediates the interaction with ECT2. As both Par6C-N and Par6C-C contain the central PDZ domain, the region of Par6 containing the PB1 and CRIB domains appeared to be critical to the binding to ECT2. To confirm the interaction, we conducted in vitro pulldown experiments with Par6 fragments fused with GST. As the in vitro binding of Par6C to ECT2 was not strong enough to analyze the binding site, we used Par6A instead. Similar to the in vivo binding results, Par6A-N1, an N-terminal fragment encompassing the PB1, CRIB, and PDZ domains (residues 1 to 191), associated with ECT2 (Fig. 3B). Moreover, Par6A-N2, which contains the PB1 and Crib domains but not the PDZ domain, was sufficient to interact with ECT2. In contrast, Par6A-C (residues 288 to 381) or GST alone did not exhibit detectable interaction with ECT2.

Par6 interacts with ECT2-C as well as ECT2-N. To define which regions of ECT2 bind to Par6 in vivo, we conducted coimmunoprecipitation assays. Myc-tagged ECT2 derivatives were expressed together with Flag-Par6A, and ECT2 was immunoprecipitated with anti-Myc antibody. As shown in Fig. 4B, both the ECT2-N derivatives, ECT2-N2 (residues 1 to 423) and ECT2-N4 (residues 1 to 319), associated with Par6. However, ECT2-N2 exhibited significantly stronger binding than ECT2-N4, suggesting that the S domain plays a supportive role in the interaction. Unexpectedly, the C-terminal half of ECT2 (ECT2-ΔN5, residues 421 to 882) also exhibited significant association with Par6. In contrast, the Myc tag alone did not show any association with Par6A. Par6C also showed similar binding to ECT2-N4, ECT2-N2, and ECT2-ΔN5 (data not shown). We also performed in vitro binding assays with GST-Par6A immobilized on glutathione beads (Fig. 4C). Interestingly, ECT2-ΔN5 bound to Par6 more strongly than ECT2-N2 in vitro. ECT2-N4 did not exhibit detectable binding to Par6 in vitro (Fig. 4C). These results suggest that the C-terminal half of ECT2 (ECT2-ΔN5) also associates with Par6, although it lacks the N-terminal domain, which was used as bait in the two-hybrid screening. Similar to Par6A, PKCζ also associated with either ECT2-N2 or ΔN5 (Fig. 2C).

To further test whether ECT2 and Par6 interact directly, we examined the binding of purified proteins. ECT2-ΔN5 was expressed as an MBP fusion protein, affinity purified, and used for binding with GST-Par6. Since GST-Par6A is very insoluble (see Fig. 1C), we used GST-Par6A-N1 protein in these assays. As shown in Fig. 4D, GST-Par6 bound specifically to the MBP-ECT2-ΔN5 fusion protein, whereas GST alone did not. MBP-ECT2-N2 also bound to GST-Par6A, albeit weakly, whereas MBP alone did not. These results suggest that the interaction of ECT2 with Par6A is direct.

Coexpression of Par6 and ECT2 efficiently activates Cdc42 and Rac1 in vivo. We previously showed that ECT2 activates RhoA, Rac1, and Cdc42 in vitro (37). Since GTP-bound Cdc42 associates with Par6 to activate aPKC, we performed pulldown assays for activated Cdc42 with a GST fusion protein contain-

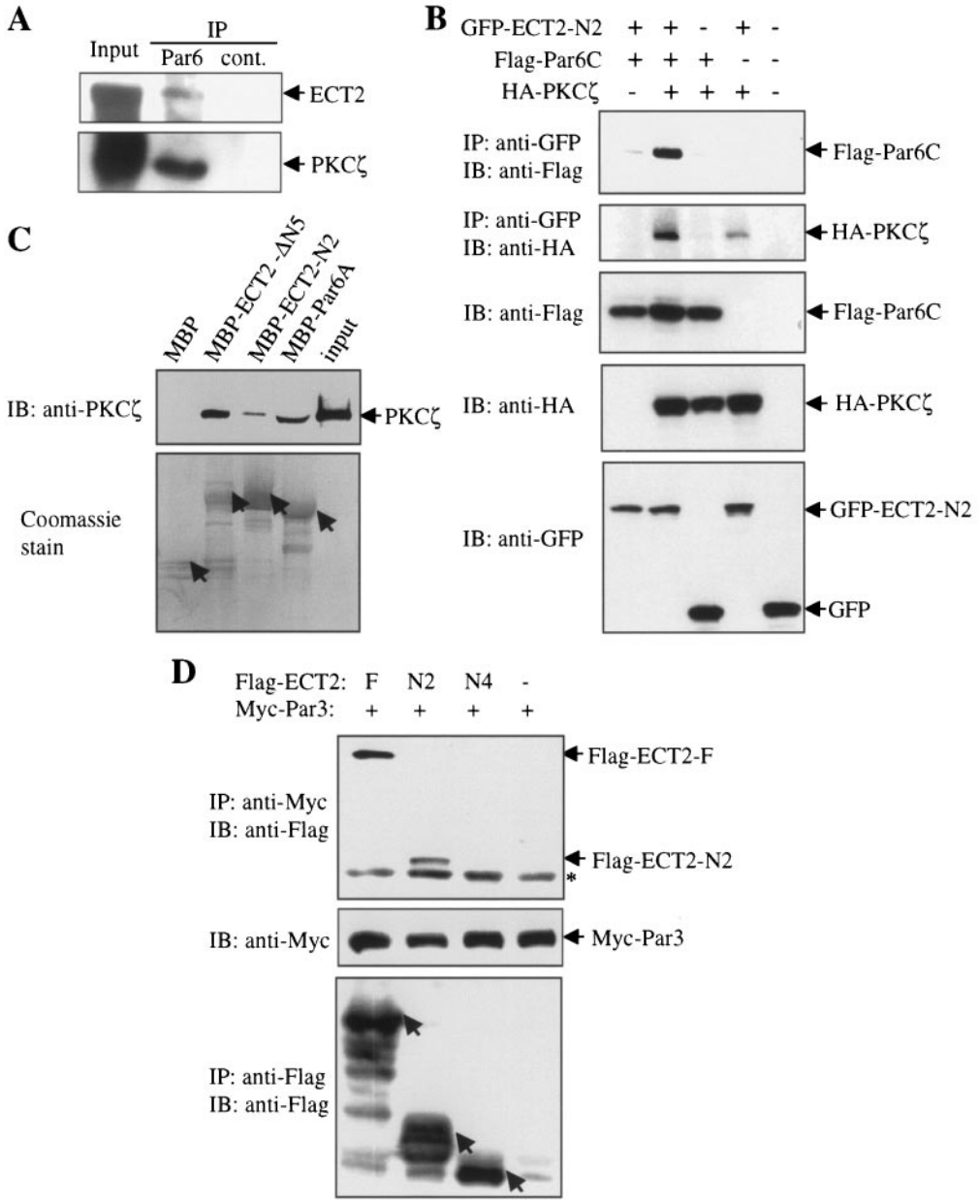

FIG. 2. ECT2 interacts with the PKCζ/Par3 complex. (A) MDCK cell lysates were subjected to immunoprecipitation with anti-Par6 (Par6) or control anti-goat antibody (cont.). Endogenous ECT2 and PKCζ were detected by immunoblotting with anti-ECT2 and anti-PKCζ, respectively. (B) ECT2 associates with Par6 and PKCζ in vivo. Cos7 cells cotransfected with GFP-ECT2-N2, Flag-Par6C, and HA-PKCζ were lysed and subjected to immunoprecipitation (IP) with anti-GFP antibody. Western blot analysis was carried out with anti-GFP, anti-Flag, and anti-HA antibodies. (C) ECT2 interacts directly with PKCζ. Purified PKCζ (800 ng; Calbiochem) was incubated with MBP, MBP-ECT2-ΔN5, MBP-ECT2-N2, or MBP-Par6A beads in PBS containing 1% Triton X-100 and 1 μg of bovine serum albumin per ml for 2 h at 4°C. The protein pulled down by the beads was detected with anti-PKCζ antibody. (D) ECT2 associates with Par3 in vivo. Cos7 cells cotransfected with the Flag-ECT2 or Myc-Par3 expression vector were lysed and subjected to immunoprecipitation (IP) with anti-Myc antibody. Western blot analysis was carried out with anti-Myc and anti-Flag antibodies.

ing the p21 binding domain (PBD) of Pak (1). However, expression of ECT2-ΔN5 alone did not significantly stimulate the accumulation of GTP-bound Cdc42 under these conditions (Fig. 5A, compare lanes 2 and 4). As Par6 associated with ECT2-C as well as with ECT2-N, we reasoned that Par6 binding might activate the catalytic activity of ECT2. When Par6 was coexpressed with ECT2-ΔN5, it greatly enhanced the accumulation of GTP-bound Cdc42 (Fig. 4A, left panel, compare lanes 1 and 2). Overexpression of Par6C alone also stimulated Cdc42, albeit to a lesser extent (Fig. 4A, compare lanes 3 and 4). Similar results were also obtained in MDCK cells, and ECT2-ΔN5 and Par6 similarly activated Rac1 (Fig. 5A, right panel).

To investigate further the role of ECT2 in activation of

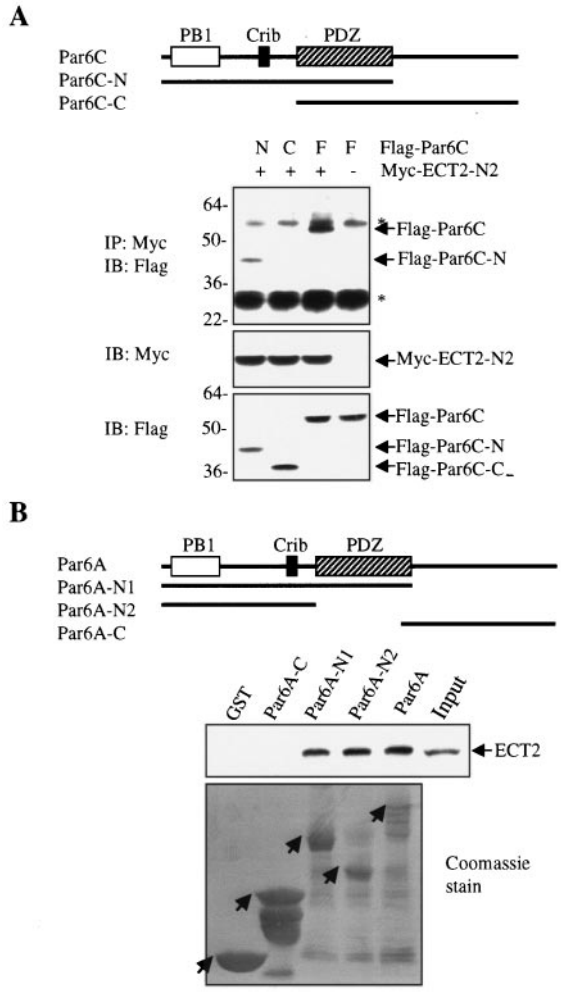

FIG. 3. N-terminal Par6 interacts with ECT2. (A) A schematic diagram of Par6C and its derivatives is shown at the top. Cos 7 cells were cotransfected with Myc-ECT2-N2 or empty Myc vector together with Par6C or its derivatives or empty Flag vector (−) as indicated. Cells were lysed, immunoprecipitated (IP) with anti-Myc antibody, and immunoblotted (IB) with anti-Flag antibody. F denotes full-length Par6C. Asterisks indicate the location of IgG light and heavy chains. The expression levels of the exogenous proteins were determined by immunoblotting with anti-Myc and anti-Flag antibodies (middle and bottom panels). (B) A schematic diagram of the domain organization of Par6A and its deletion mutants is shown at the top. Endogenous ECT2 was pulled down by GST, GST-Par6A, or its derivatives from MDCK cell lysates and detected with anti-ECT2 antibody. Arrows indicate the positions of GST fusion proteins of the expected sizes.

Cdc42, we altered the ECT2 level by using siRNAs. Consistent with previous results that perturbation of ECT2 function inhibits cytokinesis (37), multinucleated cells accumulated 48 h after siRNA transfection (data not shown). When ECT2 was knocked down by RNA interference, the GTP-Cdc42 level decreased (Fig. 5B, compare lanes 3 and 4). Moreover, overexpression of Par6 did not rescue the defect (Fig. 5B, compare lanes 1 and 3). Similar results were also observed for the GTP-Rac1 level (data not shown). These results suggest that Par6 plays a supportive role in the activation of Cdc42 and Rac1 by ECT2 in vivo.

ECT2 regulates PKCζ activity. It has been reported that overexpression of Par6 results in PKCζ activation (27). To test whether ECT2 affects PKCζ activity, we cotransfected various ECT2 derivatives together with Par6 and HA-tagged PKCζ. HA-PKCζ was immunoprecipitated with anti-HA antibody, and its kinase activity was estimated with myelin basic protein as the substrate. Consistent with the reported results (27), we observed a marginal increase in PKCζ activity after overexpression of Par6 (Fig. 5C, compare lanes 3 and 4). Interestingly, expression of full-length ECT2 strongly stimulated the PKCζ activity (lane 1). Expression of Par6 together with ECT2 further enhanced the level of PKCζ activity (lane 2). Moreover, expression of ECT2-N2, which lacks the Dbl homology catalytic domain and pleckstrin homology domain of ECT2, slightly reduced the PKCζ activity stimulated by Par6 (compare lanes 5 and 3), suggesting that ECT2-N2 can function in a dominant negative fashion. This was consistent with our previous finding that ECT2-N inhibits cytokinesis (37). Taken together, these results suggest that ECT2 stimulates PKCζ activity and that coexpression of Par6 with ECT2 further stimulates the activity.

ECT2 localizes to cell-cell junctions of MDCK cells. We previously found that ECT2 predominantly localized in the nucleus of nonpolarized cells at interphase. During cell division, ECT2 changes its localization dynamically from mitotic spindles to the midbody (37). As the above results suggested that ECT2 regulates epithelial cell polarity through Par6, we examined the subcellular localization of ECT2 in polarized MDCK cells with affinity-purified anti-ECT2 antibody. Interestingly, ECT2 was detected at the sites of cell-cell contact as well as in the nucleus and partially colocalized with the tight junction marker ZO-1 (Fig. 6A, upper panels). Subcellular localization of ECT2 was further followed at all the stages of cell division. Similar to previous observations in HeLa cells (37), nuclear ECT2 was dispersed to the entire cell after nuclear membrane breakdown and concentrated in mitotic spindles (data not shown). ECT2 was then strongly localized at the midbody during cytokinesis (Fig. 6A, lower panels). In MDCK cells, ECT2 and ZO-1 were present between mitotic cells and neighboring cells throughout all phases of cell division. These results suggest that ECT2 has an additional function besides cytokinesis regulation, and ECT2 in cell-cell junctions may be regulated in a different manner from the nuclear ECT2 in MDCK cells. Together with the localization of Par6 at cell-cell junctions (36), our findings suggest that the interaction of ECT2 and Par6 might occur physically in MDCK cells.

To test whether ECT2 regulates tight junction formation, we knocked down ECT2 in MDCK cells by RNA interference. We designed four pairs of canine ECT2 siRNAs. Whereas none of them efficiently reduced the expression level of ECT2 (data not shown), we found that the mixture of all four pairs significantly knocked down ECT2 in MDCK cells (Fig. 6B). In a population of siRNA-treated cells, junctional ECT2 was reduced as well as nuclear ECT2 (Fig. 6C). These results further support that ECT2 is localized at cell-cell junctions as well as in the nucleus in MDCK cells. Consistent with the role of ECT2 in cytokinesis, approximately 25% of the ECT2 siRNA-treated cells became binucleated 48 h after the treatment, whereas approximately 5% of the control siRNA-treated cells were binucleated. When ECT2 siRNA-treated cells were subjected to a calcium switch, tight junction formation was not signifi-

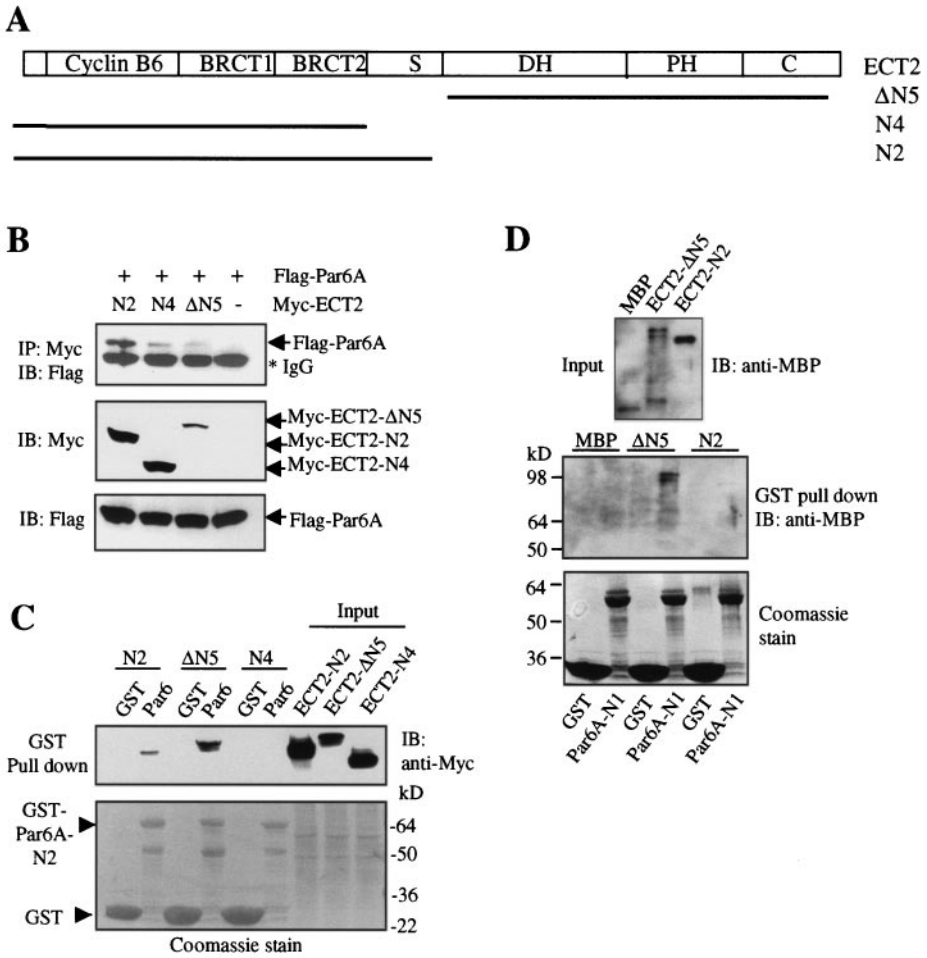

FIG. 4. Either the N- or C-terminal domain of ECT2 interacts with Par6 in vitro. (A) Schematic view of ECT2 domains and deletion mutants. (B) Interaction of ECT2 derivatives with Par6 in vivo. Cos7 cells cotransfected with Par6A and ECT2 expression vectors or vector alone (−) were subjected to immunoprecipitation (IP) with anti-Myc antibody followed by immunoblotting (IB) with anti-Flag antibody. An asterisk indicates the IgG heavy chain. The expression levels of the exogenous proteins were determined by immunoblotting with anti-Myc and anti-Flag antibodies (middle and bottom panels). (C) In vitro pulldown assays: Cos7 cells transfected with Myc-tagged ECT2-ΔN5, ECT2-N2, or ECT2-N4 were lysed, and ECT2 derivatives were pulled down by GST-Par6A or GST beads and detected with anti-Myc antibody. (D) Direct interaction of ECT2 with Par6. Purified MBP, MBP-ECT2-ΔN5, or MBP-ECT2-N2 was incubated with GST or GST-Par6A-N1 beads, and MBP fusion proteins were detected with anti-MBP antibody.

cantly affected, as detected by ZO-1 staining, compared with control siRNA-treated cells (data not shown). However, the residual ECT2 activity might be sufficient for a role of ECT2 in tight junction regulation, as ECT2 knockdown in MDCK cells was relatively inefficient.

Expression and localization of ECT2 are regulated by Ca^{2+}. MDCK cells grown in medium lacking calcium lose both tight junctions and adhesion junctions and then detach from one another (35). Readdition of calcium triggers tight junction assembly. Since ECT2 was detected in cell-cell junctions in MDCK cells, we tested whether ECT2 expression is affected by the Ca^{2+} concentration in the medium. Interestingly, the expression level of endogenous ECT2 was three to five times higher in cells growing in high-calcium medium than in cells growing in low-calcium medium, while PKCζ expression was not affected by calcium (Fig. 7A). Furthermore, upon readdition of extra calcium to adjust the concentration to that of the regular Dulbecco's modified Eagle's medium, elevation of ECT2 expression was observed (Fig. 7B). Therefore, ECT2 expression appeared to be regulated by the calcium concentration. We also examined the effects of calcium on the subcellular localization of ECT2. In low-calcium medium, ECT2 was predominantly localized in the nucleus, with no staining or faint staining at cell-cell contact sites (Fig. 7C, upper panels). In contrast, a clear localization of ECT2 in cell-cell junctions was observed in high-calcium medium (Fig. 7C, lower panels). These results suggest that the subcellular localization of ECT2 is regulated by the calcium level.

DISCUSSION

In this report, we identified the polarity determinant Par6 as a protein interacting with the guanine nucleotide exchange factor ECT2. In mammalian cells, it has been demonstrated that Par6 associates with Cdc42, Par3, and aPKC and regulates apical-basolateral polarity through the formation of epithelial

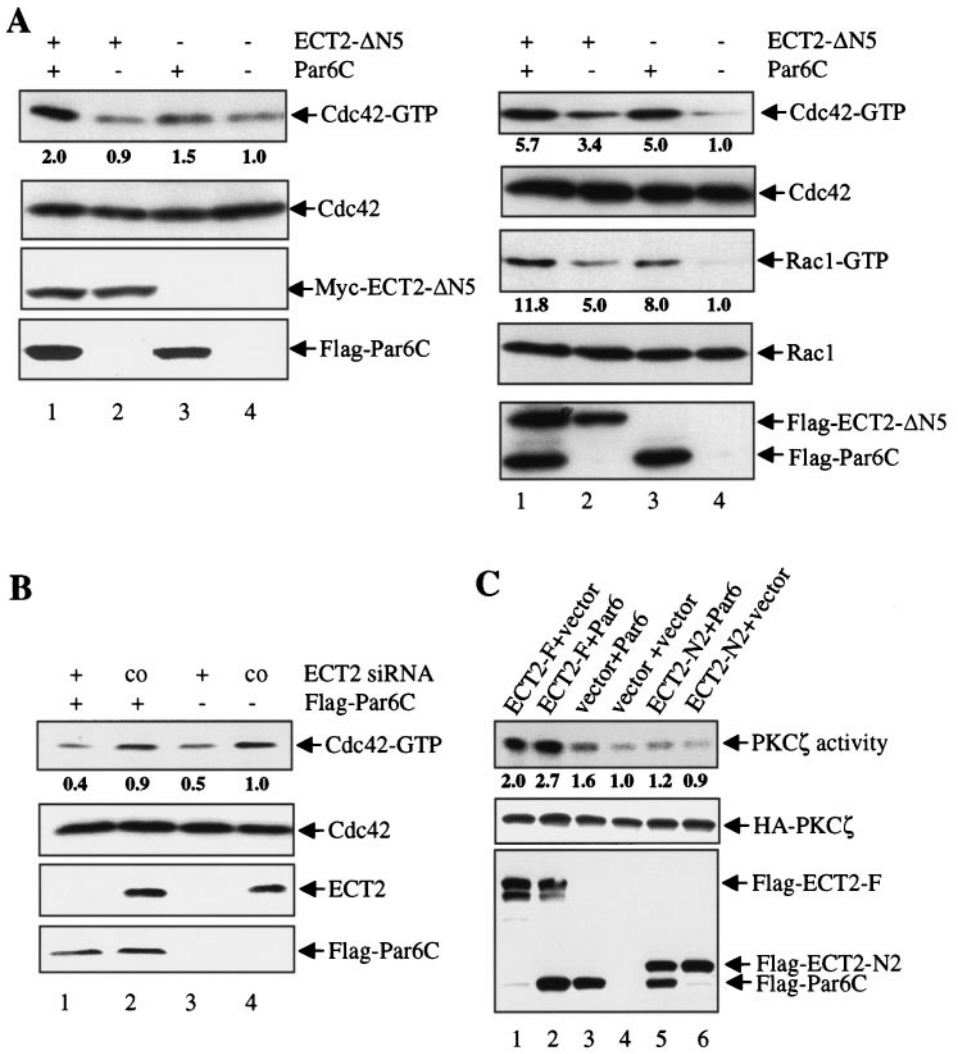

FIG. 5. Par6 and ECT2 activate Cdc42 and PKCζ. (A) (Left panel) HeLa cells transfected with Myc-ECT2-ΔN5 together with Flag-Par6C vector or vector alone were lysed, and GTP-bound Cdc42 was pulled down with GST-PBD beads. The Western blot was carried out with anti-Cdc42 antibody. (Right panel) Similar experiments were performed in MDCK cells except that Flag-ECT2-ΔN5 was used. Accumulation of GTP-bound Rac1 was also estimated (lower panel). Similar results were obtained in three independent experiments. (B) Silencing of ECT2 reduces GTP-bound Cdc42. HeLa cells were treated with ECT2 siRNA or control luciferase siRNA (co) for 5 h and then transfected with Flag-Par6C. Cells were lysed 20 h after transfection, and GTP-bound Cdc42 was pulled down with GST-PBD-Sepharose beads. Western blots were carried out with anti-Cdc42, anti-ECT2, or anti-Flag antibody. These results were reproduced in three independent experiments. (C) ECT2 stimulates PKCζ activity. Cos7 cells transfected with the HA-tagged PKCζ expression vector in combination with the ECT2 and Flag-Par6C vectors or vector alone were lysed, and HA-PKCζ was immunoprecipitated with anti-HA antibody. PKCζ activity was estimated by in vitro kinase assays with myelin basic protein as the substrate, followed by autoradiography (upper panel). The level of HA-PKCζ was detected by immunoblotting with anti-HA antibody (lower panel). X-ray-films were scanned, and signals were quantitated with NIH Image software. Data are representative of three independent experiments.

tight junctions, but its upstream regulators were largely unknown. We showed that ECT2 directly interacts with the Par6/PKCζ complex and stimulates PKCζ activity. ECT2 was localized at cell-cell junctions in MDCK cells, and silencing of ECT2 by RNA interference significantly reduced junctional ECT2 as well as nuclear ECT2.

ECT2 catalyzes guanine nucleotide exchange on RhoA, Rac1, and Cdc42 in vitro. However, we found that ECT2-ΔN5 showed little effect on activation of Cdc42 in vivo (Fig. 5). Therefore, an unknown upstream signal may be required for the stimulation of ECT2 toward Cdc42 activation. As ECT2-ΔN5 showed strong activation of Cdc42 when coexpressed with Par6, it appears that Par6 is one of the upstream regulators. It has been demonstrated that Par6 is activated by association with GTP-bound Cdc42 (10, 15, 27). Thus, ECT2 interaction with Par6 may create a positive feedback loop to amplify the signal: ECT2 activates Cdc42, Cdc42 in turn activates Par6, and then Par6 further activates ECT2. As the association of ECT2 with Par6 and PKCζ was strongly detected when all the three molecules were overexpressed (Fig. 2B) and ECT2 can associate directly with PKCζ (Fig. 2C) as well as Par6 (Fig. 4D), these proteins appear to form a ternary complex.

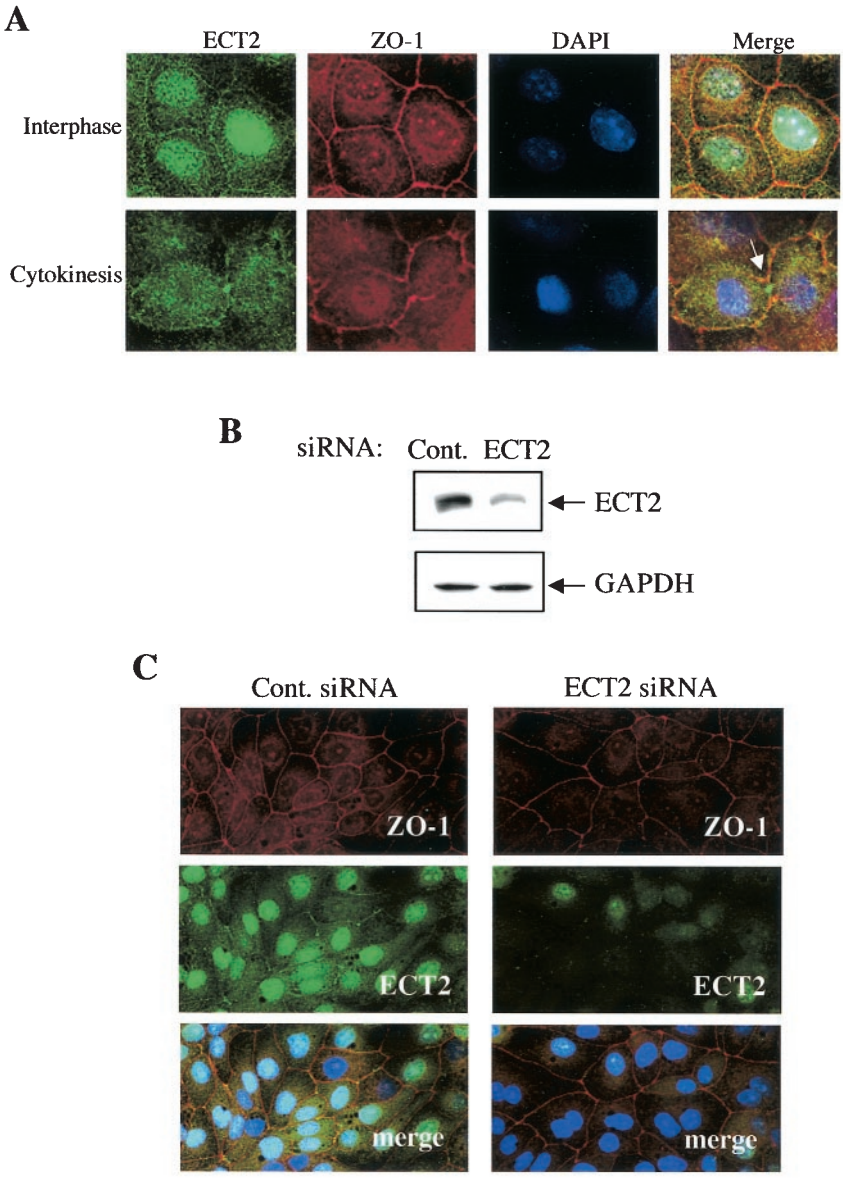

FIG. 6. ECT2 is localized at cell-cell junctions of MDCK cells. (A) Subcellular localization of ECT2 in MDCK cells. Cells were fixed with methanol and stained with polyclonal anti-ECT2 antibody (green), monoclonal anti-ZO-1 antibody (red), and 4′,6′-diamidino-2-phenylindole (DAPI) (blue for DNA). Merged pictures are shown at the right. A white arrow indicates the location of the midbody. (B and C) ECT2 expression in MDCK cells transfected with ECT2 siRNA or control luciferase siRNA. Cells were lysed 48 h after siRNA transfection, and proteins were analyzed by immunoblotting with anti-ECT2 and anti-GAPDH antibodies (B). Cells were also fixed and stained with anti-ZO-1 (red) and anti-ECT2 (green) antibodies (C). Merged staining patterns are shown with DAPI staining (blue).

We demonstrated that ECT2 associates with the Par6/PKCζ complex and enhances PKCζ activity. The stimulation appeared to be dependent upon the C-terminal catalytic domain of ECT2, as ECT2 derivatives lacking the catalytic domain did not show any stimulation of PKCζ activity (Fig. 5C). It has been reported that Par6 associates with PKCζ and stimulates its kinase activity in a Cdc42/Rac1-dependent manner (27). Thus, it is likely that ECT2 activates Cdc42 by nucleotide exchange and then GTP-bound Cdc42 associates with the Par6/PKCζ complex to stimulate PKCζ activity. Alternatively, activated Cdc42 or Rac1 may induce another signaling pathway that is independent of the polarity complex Par6/aPKC, which in turn enhances PKCζ activity. It is also possible that ECT2 stimulates PKCζ activity by directly interacting with the enzyme. A mutant form of ECT2 lacking the Par6 binding site will be useful to clarify the molecular mechanisms of PKCζ activation by ECT2.

Par6 is localized to tight junctions and/or the nucleus in polarized MDCK cells (11, 36). We found that ECT2 is partially colocalized with the tight junction marker ZO-1 in MDCK cells. The localization of ECT2 was also similar to that of the adherens junction marker β-catenin, but their localization patterns did not match exactly (data not shown). Therefore, the localization of ECT2 at the cell-cell junction was more

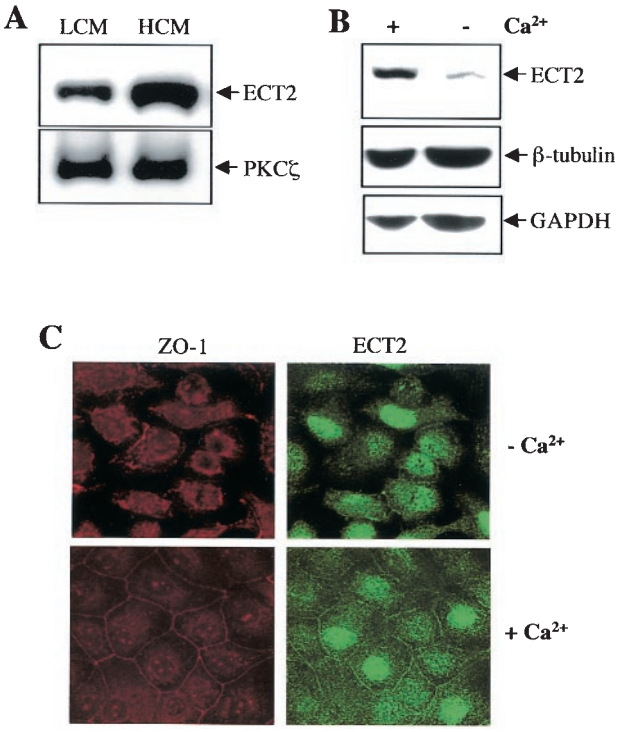

FIG. 7. ECT2 localization and expression are regulated by calcium in MDCK cells. (A) MDCK cell lysates grown in either low-calcium medium (LCM) or regular Dulbecco's modified Eagle's medium (HCM) were analyzed for ECT2 and PKCζ by Western blotting with anti-ECT2 and anti-PKC antibodies, respectively. (B) ECT2 expression was analyzed with anti-ECT2 antibody in MDCK cells grown in low-calcium medium (−) or low-calcium medium plus 200 mM calcium (+). The blot was also probed with anti-β-tubulin and anti-GAPDH antibodies to show equal protein loading. (C) Subcellular localization of ECT2 and ZO-1 was analyzed by immunostaining with anti-ECT2 and anti-ZO-1 antibodies before and after calcium addition.

consistent with that at tight junctions than at adherens junctions. We also found that ECT2 silencing by RNA interference significantly reduced junctional ECT2 as well as nuclear ECT2 in MDCK cells. These results were consistent with the observations that ECT2 was localized at cell-cell junctions as well as the nuclei.

We found that ECT2 expression was lower in cells lacking cell-cell contact sites than in cells with contact sites (Fig. 7), raising the possibility that the loss of polarity after calcium depletion is attributable to reduced ECT2 expression. ECT2 expression was induced by calcium, and its localization to tight junctions was also dependent on calcium. Cell-cell adhesion of MDCK cells is induced by calcium. When calcium is added to nonpolarized cells, ECT2 expression will be induced in addition to E-cadherin ligation, and subsequently, ECT2 will be recruited to cell-cell contact sites. The calcium-dependent expression and subcellular localization of ECT2 at cell-cell adhesion sites suggest a role of ECT2 in the regulation of tight junctions. As it has been reported that aPKC activity is required for tight junction formation (36), it is possible that ECT2 activates aPKC through Par6 at cell-cell adhesion sites. In this case, reduction of the ECT2 expression level might result in perturbation of the regulation of Par6 during tight junction formation upon a calcium switch, as Par6 negatively regulates tight junction formation (10, 16). However, ECT2 silencing by RNA interference did not significantly affected tight junction formation of MDCK cells after a calcium switch. Thus, these results did not support a major role of ECT2 in cell-cell junctions. This might be due to the inefficient knockdown level of ECT2 in MDCK cells, as cytokinesis was inhibited in only 25% of ECT2 siRNA-transfected cells. Alternatively, junctional ECT2 may play a role other than regulation of tight junction formation. Additional studies will be necessary to clarify whether ECT2 at cell-cell junctions regulates tight junction formation.

Par6 was originally identified as a polarity determinant and regulates anterior-posterior polarity through asymmetric cell division during embryogenesis in *Caenorhabditis elegans* (39). Is ECT2 involved in the determination of cell polarity during embryogenesis? Interestingly, Pebble, the *Drosophila* orthologue of the human ECT2, which is specifically required for reorganization of the actin cytoskeleton at the cleavage furrow and cytokinesis, is also required for the maintenance of asymmetric localization of Pon to the basal cell cortex to ensure its segregation into the basal daughter cell (17). Therefore, ECT2 may be a component of the general polarity regulatory complex. Further studies on ECT2 binding partners should delineate the signaling pathways towards the regulation of cell polarity and cytokinesis.

ACKNOWLEDGMENTS

We thank G. Steven Martin (U.C. Berkeley) and Ian G. Macara (University of Virginia) for plasmids and Douglas R. Lowy for support. We are grateful to Susan Garfield and Steven Wincovis (CCR Confocal Microscopy Core Facility) for technical support. We also thank Keiju Kamijo and Shin'ichi Saito for materials and technical assistance.

This work was partly supported by the Breast Cancer Think Tank Award from NIH.

REFERENCES

1. **Benard, V., B. P. Bohl, and G. M. Bokoch.** 1999. Characterization of Rac and Cdc42 activation in chemoattractant-stimulated human neutrophils using a novel assay for active GTPases. J. Biol. Chem. **274:**13198–13204.
2. **Bishop, A. L., and A. Hall.** 2000. Rho GTPase and their effector proteins. Biochem. J. **348:**241–255.
3. **Cox, D. N., S. Seyfried, L. Y. Jan, and Y. N. Jan.** 2001. Bazooka and atypical protein kinase C are required to regulate oocyte differentiation in the *Drosophila* ovary. Proc. Natl. Acad. Sci. USA **98:**14475–14480.
4. **Drubin, D. G., and W. J. Nelson.** 1996. Origins of cell polarity. Cell **84:**335–344.
5. **Etienne-Manneville, S., and A. Hall.** 2003. Cdc42 regulates GSK-3 beta and adenomatous polyposis coli to control cell polarity. Nature **421:**753–756.
6. **Etienne-Manneville, S., and A. Hall.** 2003. Cell polarity: Par6, aPKC and cytoskeletal crosstalk. Curr. Opin. Cell Biol. **15:**67–72.
7. **Etienne-Manneville, S., and A. Hall.** 2001. Integrin-mediated activation of Cdc42 controls cell polarity in migrating astrocytes through PKC zeta. Cell **106:**489–498.
8. **Hall, A.** 1998. Rho GTPase and actin cytoskeleton. Science **279:**509–514.
9. **Hurd, T. W., L. Gao, M. H. Roh, I. G. Macara, and B. Margolis.** 2003. Direct interaction of two polarity complexes implicated in epithelial tight junction assembly. Nat. Cell Biol. **5:**137–141.
10. **Joberty, G., C. Peterson, L. Gao, and I. G. Macara.** 2000. The cell polarity protein par6 links par3 and atypical protein kinase C to Cdc42. Nat. Cell Biol. **2:**531–539.
11. **Johansson, A. S., M. Driessens, and P. Aspenstrom.** 2000. The mammalian homologue of the *Caenorhabditis elegans* polarity protein PAR-6 is a binding partner for the Rho GTPases Cdc42 and Rac1. J. Cell Sci. **113:**3267–3275.
12. **Kim, S. H., L. Zhigang, and D. B. Sacks.** 2000. E-cadherin-mediated cell–cell attachment activates Cdc42. J. Biol. Chem. **275:**36999–37005.
13. **Kimura, K., T. Tsuji, Y. Takada, T. Miki, and S. Narumiya.** 2000. Accumulation of GTP-bound RhoA during cytokinesis and a critical role of ECT2 in this accumulation. J. Biol. Chem. **275:**17233–17236.

14. **Knust, E., and O. Bossinger.** 2002. Composition and formation of intercellular junctions in epithelial cells. Science **298:**1955–1959.
15. **Lin, D., A. S. Edwards, J. P. Fawcett, G. Mbamalu, J. D. Scott, and T. Pawson.** 2000. A mammalian Par-3-Par-6 complex implicated in Cdc42/Rac1 and a PKC signalling and cell polarity. Nat. Cell Biol. **2:**540–547.
16. **Lin, G., G. Joberty, and I. G. Macara.** 2002. Assembly of epithelial tight junctions is negatively regulated by par6. Curr. Biol. **12:**221–225.
17. **Lu, B., L. Ackerman, L. Y. Jan, and Y.-N. Jan.** 1999. Modes of protein movement that lead to the asymmetric localization of partner of Numb during *Drosophila* neuroblast division. Mol. Cell **4:**883–891.
18. **Madara, J. L.** 1998. Regulation of the movement of solutes across tight junctions. Annu. Rev. Physiol. **60:**143–159.
19. **Manser, E.** 2002. Small GTPases take the stage. Dev. Cell **3:**323–328.
20. **Miki, T., T. P. Fleming, D. P. Bottaro, J. S. Rubin, D. Ron, and S. A. Aaronson.** 1991. Expression cDNA cloning of the KGF receptor by creation of a transforming autocrine loop. Science **251:**72–75.
21. **Miki, T., C. L. Smith, J. E. Long, A. Eva, and T. P. Fleming.** 1993. Oncogene ECT2 is related to regulators of small GTP-binding proteins. Nature **362:** 462–465.
22. **Nakagawa, M., M. Fukata, M. Yamaga, N. Itoh, and K. Kaibuchi.** 2001. Recruitment and activation of Rac1 by the formation of E-cadherin-mediated cell–cell adhesion sites. J. Cell Sci. **114:**1829–1838.
23. **Nelson, W. J.** 2003. Adaptation of core mechanisms to generate cell polarity. Nature **422:**766–774.
24. **Petronczki, M., and J. A. Knoblich.** 2001. DmPAR-6 directs epithelial polarity and asymmetric cell division of neuroblasts in Drosophila. Nat. Cell Biol. **3:**43–49.
25. **Plants, P. J., J. P. Fawcett, D. C. C. Lin, A. D. Holdorf, K. Binns, S. Kulkarni, and T. Pawson.** 2003. A polarity complex of mPar6 and atypical PKC binds, phosphorylates and regulates mammalian Lgl. Nat. Cell Biol. **5:**301–308.
26. **Ponting, C., T. Ito, J. Moscat, M. T. Diaz-Meco, F. Inagaki, and H. Sumimoto.** 2002. OPR, PC and AID: all in the PB1 family. Trends Biochem. Sci. **27:**10.
27. **Qiu, R. G., A. Abo, and G. S. Martin.** 2000. A human homolog of the C. elegans polarity determinant Par-6 links Rac and Cdc42 to PKC signaling and cell transformation. Curr. Biol. **10:**697–707.
28. **Rojas, R., W. G. Ruiz, S.-M. Leung, T.-S. Jou, and G. Apodaca.** 2001. Cdc42-dependent modulation of tight junctions and membrane protein traffic in polarized Madin-Darby canine kidney cells. Mol. Biol. Cell **12:**2257–2274.
29. **Rolls, M. M., and C. Q. Doe.** 2003. Cell polarity—from embryo to axon. Nature **421:**905–906.
30. **Saito, S., X. F. Liu, K. Kamijo, R. Razziudin, T. Tatsumoto, I. Okamoto, X. Chen, C. C. Lee, M. V. Lorenzi, N. Ohara, and T. Miki.** 2003. Deregulation and mislocalization of the cytokinesis regulator ECT2 activate the Rho signaling pathways leading to malignant transformation. J. Biol. Chem. **279:** 7169–7179.
31. **Saito, S., T. Tatsumoto, M. V. Lorenzi, M. Chedid, V. Kapoor, H. Sakata, J. Rubin, and T. Miki.** 2003. Rho exchange factor ECT2 is induced by growth factors and regulates cytokinesis through the N-terminal cell cycle regulator-related domains. J. Cell Biochem. **90:**819–836.
32. **Sakata, H., J. S. Rubin, W. G. Taylor, and T. Miki.** 2000. A Rho-specific exchange factor Ect2 is induced from S to M phases in regenerating mouse liver. Hepatology **32:**193–199.
33. **Schmidt, A., and A. Hall.** 1999. Guanine nucleotide exchange factors for Rho GTPases: turning on the switch. Genes Dev. **16:**1587–1609.
34. **Shi, S.-H., L. Y. Jan, and J. Y.N.** 2003. Hippocampal neuron polarity specified by spatial localized mPar3/Par6 and PI3-kinase activity. Cell **112:**63–75.
35. **Siliciano, J. D., and D. A. Goodenough.** 1988. Localization of the tight junction protein, ZO-1, is modulated by extracellular calcium and cell-cell contact in Madin-Darby canine kidney epithelial cells. J. Cell Biol. **107:**2389–2399.
36. **Suzuki, A., T. Yamanaka, T. Hirose, N. Manabe, K. Mizuno, M. Shimizu, K. Akimoto, Y. Izumi, T. Ohnishi, and S. Ohno.** 2001. Atypical protein kinase C is involved in the evolutionarily conserved par protein complex and plays a critical role in establishing epithelia-specific junctional structures. J. Cell Biol. **152:**1183–1196.
37. **Tatsumoto, T., X. Xie, R. Blumenthal, I. Okamoto, and T. Miki.** 1999. Hum. ECT2 is an exchange factor for Rho GTPases, phosphorylated in G2/M phases, and involved in cytokinesis. J. Cell Biol. **147:**921–927.
38. **Vania, M., and M. Braga.** 2002. Cell-cell adhesion and signalling. Curr. Opin. Cell Biol. **14:**546–556.
39. **Watts, J. L., B. Etemad-Moghadam, S. Guo, L. Boyd, B. W. Draper, C. C. Mello, J. R. Priess, and K. J. Kemphues.** 1996. par-6, a gene involved in the establishment of asymmetry in early *C. elegans* embryos, mediates the asymmetric localization of PAR-3. Development **122:**3133–3140.
40. **Whitehead, I. P., S. Campbell, K. Rossman, and C. J. Der.** 1997. Dbl family proteins. Biochim. Biophys. Acta **1332:**F1–F23.
41. **Wodarz, A.** 2002. Establishing cell polarity in development. Nat. Cell Biol. **4:**E39–E44.
42. **Yamanaka, T., Y. Horikoshi, A. Suzuki, Y. Sugiyama, K. Kitamura, R. Maniwa, Y. Nagai, A. Yamashita, T. Hirose, H. Ishikawa, and S. Ohno.** 2001. PAR-6 regulates aPKC activity in a novel way and mediates cell-cell contact-induced formation of the epithelial junctional complex. Genes Cells **6:**721–731.
43. **Yamanaka, T., Y. Horikoshi, Y. Sugiyama, C. Ishiyama, A. Suzuki, T. Hirose, A. Iwamatsu, A. Shinohara, and S. Ohno.** 2003. Mammalian Lgl forms a protein complex with PAR-6 and aPKC independently of PAR-3 to regulate epithelial cell polarity. Curr. Biol. **13:**734–743.